

UV-cured powder transparent coatings based on oligo(meth)acrylic resins

Katarzyna Pojnar^{1), *} (ORCID ID: 0000-0001-9877-7448), Barbara Pilch-Pitera²⁾ (0000-0002-2412-2219), Maciej Kisiel³⁾ (0000-0003-2034-9026), Aleksandra Zioło¹⁾ (0000-0003-3833-0673), Michał Kędzierski⁴⁾ (0000-0002-5812-6525)

DOI: <https://doi.org/10.14314/polimery.2024.1.2>

Abstract: Polyacrylic resins containing glycidyl methacrylate (GMA), methyl methacrylate (MMA) and n-butyl acrylate (BA) in various molar ratios were obtained. Triaryl sulfonium hexafluorophosphate was used as a photoinitiator and reacted with the epoxy groups of GMA. The relationship between the chemical structure of polyacrylic resins and the parameters of the UV curing reaction and the functional properties of powder coatings was investigated. The appearance and mechanical properties of the coatings were determined based on thickness, gloss, roughness, deformability, scratch resistance, adhesion to steel, hardness, and water contact angle. DMA was used to assess the cross-link density. Powder coatings with good physical and mechanical properties and curing time of 70 s were obtained.

Keywords: polyacrylic resins, powder varnishes, UV curing, cationic photopolymerization.

Utwardzane UV lakiery proszkowe na bazie żywic oligo(metylo)akrylowych

Streszczenie: Otrzymano żywice poliakrylowe zawierające metakrylan glicydyli (GMA), metakrylan metylu (MMA) i akrylan n-butylu (BA) w różnych stosunkach molowych. Jako fotoinicjatora użyto heksafluorofosforanu triarylosulfoniowego, który reagował z grupami epoksydowymi GMA. Zbadano zależność pomiędzy budową chemiczną żywic poliakrylowych a parametrami reakcji utwardzania UV i właściwościami użytkowymi powłok proszkowych. Wygląd i właściwości mechaniczne powłok określano na podstawie grubości, połysku, chropowatości, odkształcalności, odporności na zarysowania, przyczepności do stali, twardości i kąta zwilżania wodą. Do oceny gęstości usieciowania zastosowano DMA. Otrzymano powłoki proszkowe o dobrych właściwościach fizyko-mechanicznych i czasie utwardzania 70 s.

Słowa kluczowe: żywice poliakrylowe, lakiery proszkowe, utwardzanie UV, fotopolimeryzacja kationowa.

Ecology is one of the fundamental aspects of the development of new technologies. Environmental regulations in Europe try to reduce, among others, emissions of volatile organic compounds (VOCs) in liquid paints. The emission of toxic compounds to the environment contributes to global warming. Powder coatings do not contain VOCs. They also do not require the use of in-can biocides

(necessary for water-based products), thus fulfilling an important environmental aspect [1]. Powder coatings not only reduce the emission of VOCs, but also limit the generation of waste compared to liquid products. UV-cured powder coatings also makes possible to reduce energy consumption because it is necessary to heat the coating only to melt the powder (approx. 100–120°C), while the crosslinking reaction is initiated by UV radiation, not thermally (160–200°C) as in the case of classic powder coatings [2, 3]. Johansson *et al.* [4] showed the advantages of using photoinitiation compared to thermal initiation and presented solutions associated with oxygen inhibition. In their research, they used a mixture of an amorphous methacrylate-functional prepolymer and crystalline acrylate and methacrylate. The UV-curing reduced the effect of oxygen inhibition and simplified the melting process. In addition, recent research by Johansson *et al.* were focused on bio-based UV-cured powder coatings such as limonene-derived polycarbonates, which contribute to meeting the principles of sustainable development.

¹⁾ Doctoral School of Engineering and Technical Sciences at the Rzeszow University of Technology, ul. Powstańców Warszawy 12, 35-959 Rzeszów, Poland.

²⁾ Faculty of Chemistry, Department of Polymers and Biopolymers, Rzeszow University of Technology, ul. Powstańców Warszawy 6, 35-959 Rzeszów, Poland.

³⁾ Faculty of Chemistry, Department of Industrial and Materials Chemistry, Rzeszow University of Technology, ul. Powstańców Warszawy 6, 35-959 Rzeszów, Poland.

⁴⁾ Łukasiewicz Research Network – Industrial Chemistry Institute, ul. Ludwika Rydygiera 8, 01-793 Warsaw, Poland.

^{*} Author for correspondence: d521@stud.prz.edu.pl

Nevertheless, these solvent coatings emit VOCs [5]. The following advantage of UV-curing is the short reaction time which gives additional energy benefits. Due to the milder conditions of UV-cured powder coatings formation, they can be used on heat-sensitive substrates, such as medium-density fiberboard (MDF), wood or plastic. For this reason, UV-curing processes are attractive in a wide range e.g.: printing inks, microelectronics, dental repair, adhesives, biological materials, and coatings [6].

Photopolymerization begins with photon absorption by the photoinitiator, whereby the photoinitiators excited state is achieved. After absorbing energy, the photoinitiator decays to form reactive ions or free radicals. Reactive molecules (ions or free radicals) react with the monomer (M) initiating the growing chain of polymer (Fig. 1) [7]. This technique involves converting a liquid mixture of monomers or oligomers into a solid three-dimensional polymer network [8].

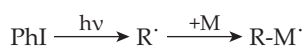


Fig. 1. Scheme of photoinitiated polymerization (PhI – photoinitiator, R – free radical or ion, M – monomer molecule, R-M – initiated polymer chain) [8]

Currently, two types of UV-curing cross-linking process of coatings are used: free radical photopolymerization (e.g. in the case of (meth)acrylic and unsaturated polyesters) or cationic-initiated chain-growth polymerization (e.g. polymerization of epoxides and vinyl ethers) [8, 9]. In free radical photopolymerization, the main problem is caused by atmospheric oxygen, which slows down or even stops the initiation process. During UV-curing, oxygen reacts with the photoinitiator in excited state, deactivating it. In contrary, the cationic photopolymerization reaction, is characterized by the absence of oxygen inhibition and the possibility of a reaction after removal of the radiation source, the so-called dark curing [10]. The development of UV-cured powder transparent coatings cured by cationic photopolymerization can also give a new approach to the powder coatings market.

Recently, many scientists have conducted research on UV curing process. The UV-cured acrylic systems can be used for modification of e.g. polyurethanes, epoxy, and unsaturated polyester resins [11–14]. Czachor-Jadacka *et al.* developed synthesis methods of new crosslinking agents based on urethane acrylic for unsaturated polyester resins, for free radical UV-cured powder coatings. The powder coatings crosslinked using the developed urethane-acrylic were characterized by high hydrophobicity and scratch resistance [11]. Wenning *et al.* described a UV radiation-cured powder composition, that contains amorphous urethane acrylate, which is stable to light and weathering, flexible, hard, and possesses good adhesion to steel panels [12]. Hammer *et al.* described urethane methacrylate's as reactive crosslinking agents for free radical UV-cured polyester powder coatings. They consist of methacrylate polyester resin (MPE resin), reactive

crosslinking agents, photoinitiators (Irgacure 184 and Irgacure 819), benzoin and Modaflow 6000. The reactive urethane methacrylate in the formulation caused a significant reduction in the viscosity of the melt during the crosslinking process and increased glass transition temperature, crosslinking density, and impact resistance after curing. [13]. UV-cured epoxy acrylic are inexpensive compared to other oligomers and, after cationic polymerization, show excellent adhesion to a variety of substrates, good chemical and corrosion resistance, excellent electrical insulation, high tensile, flexural, and compressive strength with thermal stability. Rawar *et al.* designed sprayable solvent-borne coatings based on epoxy acrylate, reactive diluents, photoinitiators and functional additives, which were cured within 10 s of UV exposure and exhibited excellent thermal and stain resistance properties [14]. Nevertheless, solvent-borne coatings are characterized by high VOCs emission. The disadvantages of epoxy acrylic are low flexibility and poor resistance to yellowing [15]. In addition, acrylic resins have low thermal resistance. Chebil *et al.* described the thermal degradation of methyl methacrylate resin-based materials known as ELIUM[®] resin. Degradation was observed above 180°C temperatures, even with the use of antioxidants [16]. As mentioned earlier, standard thermosetting powder coatings are cured above 180°C. The UV-curing method does not need such high temperatures compared to thermosets systems. For this reason, UV curing allows the use of oligo(meth)acrylic resins in powder coatings, thus not impairing their physical and chemical properties. Examples of commercial UV-cured powder coatings are acrylic resins of Uvecoat 2000, 2100, and 2200 series, developed by Allnex company [17]. They are characterized by good adhesion and protect properly pre-treated substrates against corrosion.

Due to the excellent properties of the coatings obtained from UV-cured acrylic resins, it seems justified to continue scientific research to better understand the dependence of the influence of their structure on the coating properties. This may result in coatings with improved performance, in particular flexibility and impact resistance without losing storage. For this reason, as part of this work, an attempt was made to modify UV-cured epoxy functional acrylate resins by using monomers with different chemical structures and different molar ratios to optimize coating properties.

The aim of this work was to investigate the relationship between the chemical structure of oligo(meth)acrylic resins and the UV curing process conditions on the properties of powder coatings. Clarification of these relationships is necessary to develop coatings with better properties. The gel permeation chromatography (GPC), differential scanning calorimetry (DSC) and Brookfield viscosity measurements were used to determine the rheology parameters of the oligo(meth)acrylic resins. The structure of oligo(meth)acrylic resins was confirmed by ¹H-NMR (nuclear magnetic resonance) and FT-IR

(Fourier-transform infrared spectroscopy) spectra. The crosslinking bonds created in the polymerization reaction of the epoxy groups derived from glycidyl methacrylate (GMA) initiated by triaryl sulfonium hexafluorophosphate photoinitiator were identified by using dynamic mechanical analysis (DMA). In addition, thickness, gloss, roughness, cupping, scratch resistance, adhesion to the steel, hardness and water contact angle were determined to evaluate the coating performance properties.

EXPERIMENTAL PART

Materials

Glycidyl methacrylate (GMA) $\geq 97.0\%$ (GC), methyl methacrylate (MMA) $\geq 99\%$, stabilized, *n*-butyl acrylate (BA) $\geq 99\%$, contains 10–60 ppm monomethyl ether hydroquinone as inhibitor and free radical initiator of polymerization: azobisisobutyronitrile $\geq 98\%$, (AIBN) obtained from Sigma Aldrich (Taufkirchen, Germany) were used for the synthesis of oligo(meth)acrylic resins.

Photoinitiator – triaryl sulfonium hexafluorophosphate 50 wt% in propylene carbonate obtained from Sigma Aldrich (Taufkirchen, Germany), degassing agent – benzoin, purified by sublimation, $\geq 99.5\%$ obtained from Sigma Aldrich (Buchs, Switzerland) and flow control agent: Byk 368P obtained from Byk (Wesel, Germany) were used for the UV-cured powder transparent coatings preparation as raw materials.

Other reagents used in research are tetrahydrofuran HPLC grade, chloroform, glacial acetic acid, tetraethylammonium bromide and perchloric acid, obtained from Sigma Aldrich (Taufkirchen, Germany).

Synthesis of acrylic resins

An appropriate amount of glycidyl methacrylate, methyl methacrylate, *n*-butyl acrylate and 1.7 wt% azobisisobutyronitrile were placed in a three-necked flask equipped with a reflux condenser, a thermometer, a magnetic stirrer, and a nitrogen inlet (the reaction is sensitive to oxygen inhibition). Azobisisobutyronitrile was used as an initiator, which was added directly to the mono-

mers. Due to the lack of oxygen in the initiator, the resulting product does not undergo oxidation and yellowing reactions [18]. The reaction mixture was then maintained at the temperature of 80°C stirred and refluxed for one hour. Polymerization reactions began when the viscosity increased rapidly. Next, the not solidified mixture of resin was poured onto PTFE (polytetrafluoroethylene) mold for solidification. To complete the polymerization process, the PTFE mold with the resin was sealed and placed in an oven at 80°C for one hour. Finally, the mold was cooled, and the solidified resin was ground. The obtained resins were named according to the molar ratio and names of the monomers used, e.g. GMA/6MMA/1BA means a resin made from the GMA, MMA, and BA monomers in molar ratio of 1:6:1.

Preparation of UV-cured powder transparent coatings

For obtaining UV-cured powder transparent coatings 2 or 4 wt% photoinitiators (triaryl sulfonium hexafluorophosphate), 1 wt% benzoin and 2 wt% Byk 368P relative to the total weight of the composition were mixed. The prepared mixture was grinded and extruded in a co-rotating twin screw mini extruder EHP 2 x 12 Sline from Zamak Mercator (Skawina, Poland). The temperature in the extruder was as follows: zone I – 95°C, zone II – 110°C, zone III – 120°C and adapter – 125°C. The screw's rotational speed was 100 rpm. After extrusion, the mixture was cooled, pulverized, and sieved in a 100 μm sieve. Metal plates were appropriately prepared before application. The surface of the metal plates was cleaned, degreased, and passivated using zirconium phosphate conversion coating ESKAPHOR Z 2000C from Haug Chemie (Sinsheim, Germany). The resulting powder coatings were applied to the metal plates, wood and MDF. The powder coatings were applied by electrostatic gun PEM X-1 controlled by EPG Sprint X (CORONA) from Wagner (Allstate, Switzerland). The coatings were melted at 130°C for 5 minutes. Then, the coatings were cured using a Dymax UVC-5 Compact Light-Curing Conveyor System equipped with a mercury lamp (Wiesbaden, Germany). The number of cure cycles varied depending on the glycidyl methacrylate (GMA) molar ratio. The UV-curing process is shown in Figure 2.

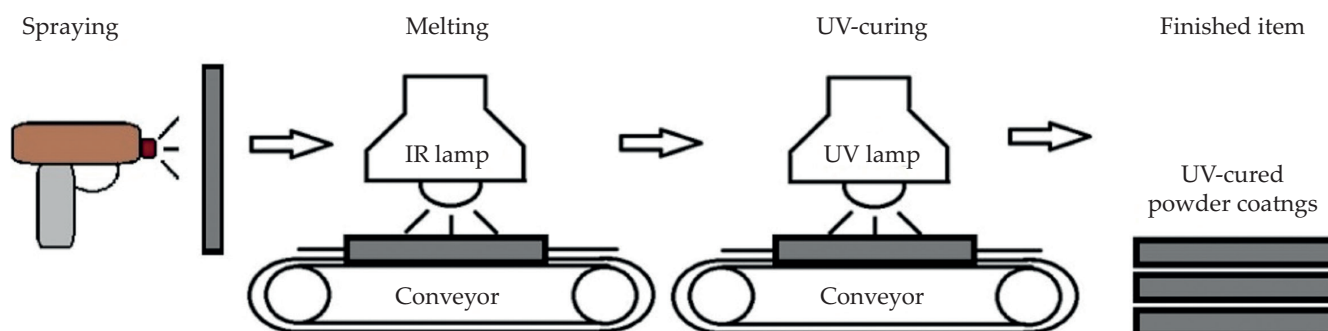


Fig. 2. Scheme of the line for obtaining UV-cured powder coatings

The obtained powder coatings were named according to the names of the resin used, e.g. L_GMA/6MMA/1BA means a coating made from the resin GMA/6MMA/1BA.

Measurements

Characterizations of oligo(meth)acrylic resins

Gel permeation chromatography

The gel permeation chromatography (GPC) equipped with the RI detector Shodex RI-71, the Shimadzu LC-20AD isocratic pump (Kyoto, Japan), the ViscoTec (Töging, Germany) degassing system, a PSS SDV guard column and PSS SDV 100, 1000, 10000Å columns with a grain diameter of 5 µm, packed with styrene divinylbenzene-type gel were used. All samples were dissolved in tetrahydrofuran (HPLC grade) in a temperature of 22°C. The interpretation of results was based on the conventional calibration of columns with polystyrene standards. Calibration solutions were prepared by dissolving 1–1.5 mg of a standard in 1 ml of tetrahydrofuran (THF). Solutions before analysis were shaken for 24 h at ambient temperature and then filtered through syringe filters with the diaphragm (PTFE) 0.25 µm.

¹H NMR spectroscopy

The nutransparent magnetic resonance (¹H NMR) spectra were recorded with a Bruker Avance II 500 MHz (Billerica, USA). This instrument was equipped with a 5 mm nitrogen-cooled dual (BB-1H) cryoprobe. Tetramethylsilane was used as an internal standard. The units of the chemical shift values were ppm. During the study, deuterated chloroform (CDCl₃) was used as a solvent. NMR Topspin 2.1 pl 8 software was used.

FT-IR spectroscopy

To determine the chemical structure of acrylic resin, the Thermo Scientific Nicolet 6700 FT-IR spectrophotometer (Waltham, USA) was used. The relations between transmittance and the wavenumber were recorded in the range of 700–4000 cm⁻¹ with a resolution of 4 cm⁻¹.

Viscosity

The viscosity of the resin was measured at 140°C using a cone-plate CAP 2000+ Brookfield viscometer (Labomat, Saint Denis Cedex, France) equipped with a cone no. 6, according to PN-EN ISO 2884-1.

Differential scanning calorimetry

Thermal properties of powder compositions were investigated using a Mettler Toledo 822° calorimeter equipped with Star^e System software (Milano, Italy). The calibration of the DSC apparatus was carried out using indium and zinc standards supplied by Mettler Toledo. The samples (10 mg) were weighed with an accuracy of 0.01 mg, following were hermetically sealed in standard 40 µL aluminum crucibles and placed in the mea-

suring chamber. The measurements were taken in the temperature range from 0 to 200°C, in a heating rate of 20°C/min, in the atmosphere of nitrogen with a flow rate of 60 mL/min.

Thermogravimetric analysis

Thermogravimetric analysis was performed using a Mettler Toledo TGA/DSC1 thermobalance with the Stare System software. The TG experiments have been carried out in nitrogen from 25 to 600°C, at heating rate of 10°C/min. The measurement conditions were as follows: sample weight ~ 6 mg, gas flow 50 mL/min, and 150 µL open alumina pan.

Determination of the epoxy equivalent weight of the oligo(meth)acrylic resin

Determination of epoxy equivalent weight of the oligo(meth)acrylic resin was carried out according to PN-EN ISO 3001. A resin containing 0.6 to 0.9 mmol of epoxy groups was weighed (with an accuracy of 0.1 mg) and placed in 100 mL Erlenmeyer flask. Then, 10 mL of chloroform was added, in which the sample was dissolved. After the resin dissolution, 20 mL of glacial acetic acid, 10 mL of tetraethylammonium bromide and a few drops of crystal violet were added (3–5 drops of violet indicator). The sample was titrated with 0.1 M chloric acid (VII) solution until it turned green. A blank test was also performed.

The epoxy equivalent weight was calculated according to the Equation 1:

$$EEW = \frac{1000 \cdot m}{(V_1 - V_0) \cdot \left(1 - \frac{t - t_s}{1000}\right) \cdot c} \quad (1)$$

where: m – mass of analytical sample (g), V_0 – volume of 0.1 M chloric acid (VII) used to titration the blank sample (mL), V_1 – volume of 0.1 M chloric acid (VII) used to titration of the test sample (mL), t – temperature of 0.1 M chloric acid (VII) during the determination (°C), t_s – temperature of 0.1 M chloric acid (VII) during titration setting (°C), c – concentration of 0.1 M chloric acid (VII) during titration setting (mol/dm³).

Characterizations of powder transparent coatings

Polymerization test

The polymerization test was evaluated based on the guidelines in the “Technical requirements of the QUALICOAT quality label” [19]. The sample was assessed 30 minutes after rubbing of the coatings with a swab soaked in MEK (methyl ethyl ketone) 30 times in each direction, and classified according to the following criteria: 1) the coating is matt and soft, 2) the coating is matt and can be scratched with a nail, 3) slight loss of gloss, 4) no noticeable changes.

The polymerization test was performed twice for each coating.

Dynamic mechanical analysis

Dynamic mechanical analysis (DMA) measurements were carried out by using DMA/SDTA861e unit from Mettler Toledo (Milano, Italy). In this analysis were used compressing mode at a constant frequency: 1Hz, in the range of temperature: 0–200°C (heating rate 3°C/min), force amplitude: max. 0.4 N and displacement amplitude: max. 2.5 µm. The samples were formed under a SPECA hydraulic press (sample diameter approximately 15 mm, thickness 2.5 mm, geometry factor 14,15 1/m and weight 0.5 g). Then, the samples were melted at 130°C for 5 minutes and cured in a UV lamp (Dymax UVC-5).

Polarized optical microscopy

LAB 40M optical microscope (Opta-tech, Warsaw, Poland) was used. Observations were made with reflected light (5W LED light) in the bright field technique and polarized light. The movement precision of focus adjustment was 0.002. To examine the coated substrates, objective 20× was used. The images were taken at a resolution 3072 × 2048 (total pixels 2675 µm). The measurements were made using the computational imaging software Capture V2.3.

Thickness and gloss

The test was carried out using a gloss meter micro-Tri-gloss-µ with thickness measurement function by BYK-Gardner (Geretsried, Germany) according to the standards: PN-EN ISO 2813 (for gloss) and PN-EN ISO 2808 (for thickness). The gloss was examined by measuring the intensity of light reflected from the coating at an incident angle of 60°. The thickness analysis was performed by the same device, which has a built-in Fe/NFe sensor. Gloss and thickness results were averaged from ten measurements for each sample.

Roughness

Measurements were made at a LT=5600 mm and LC=0.800 x5N using a Mar SurfPS1 apparatus from Mahr GmbH (Göttingen, Germany), according to the PN-EN ISO 12085 standard. The test indicated two roughness parameters R_a and R_z . The parameter R_a means the arithmetic mean deviation from the baseline expressed in µm and R_z means the arithmetic mean of the five highest profile hills decreased by the arithmetic mean of the five lowest profile depths. The roughness results were determined at ten separate locations on the surface of the same coating and the average of ten measurements was taken as the result.

Pressability

Pressability tests were carried out using a manual SP4300 tester by TQC (Capelle aan den IJssel, Netherlands) according to the PN-EN ISO 1520 standard. The tests consisted of pressing a spherical drawing punch into a clamped sheet until a crack appeared. To check the repeatability of the results, three measurements of the same cured coating were performed.

Scratch resistance

The scratch resistance test Elcometer 3000 Manual Clemen Unit (Manchester, England) was conducted in accordance with the PN-EN ISO 1518 standard. The cured coating was placed on test table, which moved with increasing loads on the needle until the coating was scratched. After scratching, the needle load value was read. The measurements were repeated four times with the same composition.

Adhesion to the steel

The test of adhesion to the steel was carried out according to the PN-EN ISO 2409 standard using a multi-cut tool manufactured by BYK-Gardner (Wesel, Germany). The cross-cut method was applied using a special multi-cut tool equipped with six cutters. The cuts were made perpendicular to each other, creating a grid of squares, with the spacing of 2 mm. The dust produced during the cutting was brushed off the surface of the coating, by use brush. Additionally, an adhesive tape was used with a width of 50 mm and a standardized peel force (glue). After the tape was broken, the appearance of the mesh was evaluated. The surface of coatings was examined with the naked eye and classified using 0–5 six-point scale, where zero represented no traces other than knife marks and five being almost complete or complete detachment of the coating. The test was repeated twice for the same coating.

Hardness

Measurements of the coating hardness were conducted according to the standard PN-EN ISO 1522 using König Pendulum ASTM D4366 manufactured by BYK-Gardner (Geretsried, Germany). The relative hardness was calculated by dividing the arithmetic mean of the number of pendulum oscillations for the tested sample by glass constant, which is 171 pendulum oscillations. Three measurements were made for the same coating.

Water contact angle

Water contact angle (CA) was determined according to the standard EN 828 using optical goniometer OCA15 EC manufactured by Data Physics (Filderstadt, Germany). The drop contours were measured using the SCA20U computer software and the contact angle was calculated. Measurements were made at ten separate locations on the surface of the same coating. The result was averaged.

RESULTS AND DISCUSSION

The properties of the powder paint determine its application, efficiency, method of application, thickness of the coating and the speed of the curing process. The application of powder coating is determined by its physical properties, chemical structure of the raw materials and the wavelength absorbed by photoinitiator. On the other hand, the selection of resin and photoinitiator is deter-

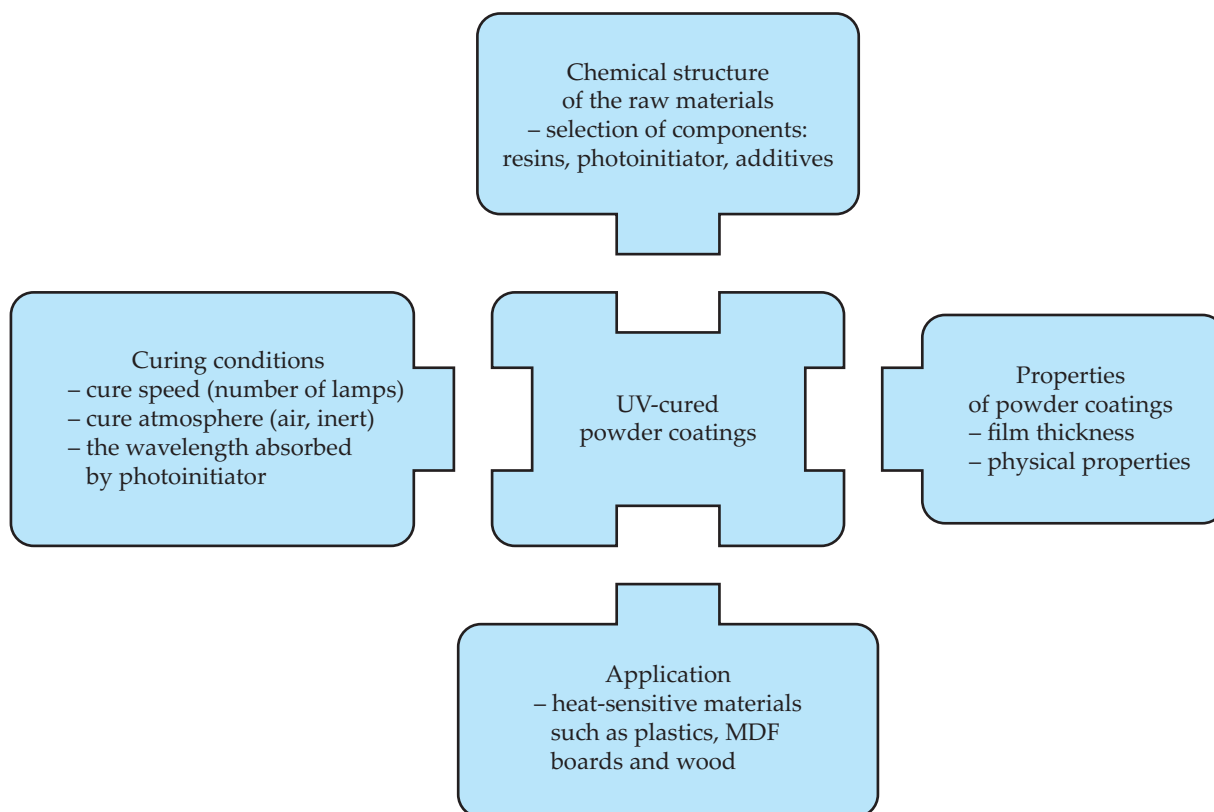


Fig. 3. Interaction between chemical structure, composition, processing parameters, coating properties and application of powder coatings

mined by the parameters of the powder coating equipment: UV energy, spectral wavelength distribution, cure speed (number of lamps) and cure atmosphere (air, inert) [20]. All these parameters and processes should be properly matched to each other to create a product with the desired properties. Relationships between mentioned properties were illustrated in Figure 3.

The selection and optimization of all these parameters is significant for obtaining UV-cured powder coatings, that have required properties and applications. For these reasons, this paper describes the effects of chemical structure of oligo(meth)acrylic resins and the parameters associated with UV-curing reaction on the properties of powder coatings and their application.

Characterization of oligo(meth)acrylic resins

Generally, acrylic resins show photostability and are resistant to hydrolysis [21]. Their disadvantage is too low flexibility, which reduces impact and cupping resistance as well as adhesion to the substrate. For this reason, *n*-butyl acrylate was added to the syntheses of acrylate resins. A four-carbon aliphatic chain influenced the flexibility of the composition and improved the cupping, adhesion, and gloss properties of powder coatings. However, a too high content of BA can lead to agglomeration of powder particles and a decrease in the stability of the powder coating during storage. Methyl methacrylate was used to increase the thermostability and

stiffness properties of the acrylic resin. The presence of a methyl group ($-\text{CH}_3$) in the main chain, at the α position to the carbonyl group, increases hydrolytic resistance compared to acrylate monomers. Glycidyl methacrylate was the major component used in the synthesis. The epoxy groups of GMA reacted with the photoinitiator and formed the crosslinked structure of the powder transparent coatings. The composition of the synthesized oligo(meth)acrylic resins is shown in Table 1. For the first four resins, the amount of GMA was constant, as the relationship between the monomers *n*-butyl acrylate and methyl methacrylate and the properties of the resulting powder transparent coatings was established. After choosing the molar ratio of *n*-butyl acrylate and methyl methacrylate, the effect of the molar ratio of GMA on the resin properties was investigated. The influence of GMA molar ratio on the crosslinking density was analyzed by DMA.

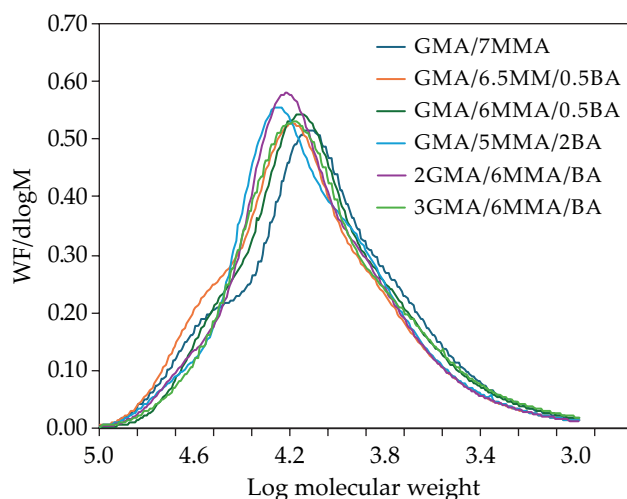
The control of the molecular mass distribution and dispersity of the synthesized resins are also very important, because acrylic monomers are more reactive. Reactivity of monomers increases according to the following order: acrylic > methacrylic > vinyl \gg allyl [20]. In this study, oligo(meth)acrylic resins were obtained, which were characterized by slightly different values in a number-average molecular mass (M_n), weight average molecular mass (M_w) and dispersity index values (D). M_n is in the range of 7 400–8 300 Da (Table 2). These values may result from not too drastic differences between the molar

T a b l e 1. The qualitative and quantitative composition of the synthesized acrylic resins

Sample	GMA mol	MMA mol	BA mol
GMA/7MMA	1.0	7.0	-
GMA/6.5MMA/0.5BA	1.0	6.5	0.5
GMA/6MMA/BA	1.0	6.0	1.0
GMA/5MMA/2BA	1.0	5.0	2.0
2GMA/6MMA/BA	2.0	6.0	1.0
3GMA/6MMA/BA	3.0	6.0	1.0

ratios of monomers used in the compositions. A high average molecular weight and low dispersity are desirable because it facilitates the formulation of powder coatings. Almost all acrylic resins are characterized by low dispersity index (below 2.0). The exception was GMA/5MMA/2BA resin. The broad polydispersity (\bar{D}) is problematic for powder coatings because powder may be unstable and stick together during storage or spraying. The major factors affecting M_n are initiator concentration, temperature, and monomers concentration [22]. Higher initiator concentrations and higher temperature can increase the amount of formed free radicals, which can also cause a termination reaction through recombination. As a result, it gives lower M_n and M_w . A higher concentration of monomer increases the growth of the polymer chain, which causes an increase in the molecular mass distribution. In this study, optimized initiator concentration (0.14 mol) and temperature (kept at 80°C for one hour) were fixed. The concentration of the respective monomers used to synthesize the resin was varied to select the sample with the best performance.

The type of monomer used also influences the molecular mass distribution e.g. in polymerization of poly(methyl methacrylate) (PMMA) and poly(methyl acrylate) (PMA). The free radical polymerization for PMMA is sterically hindered. Therefore, termination by recombination is impeded, while termination by disproportionation dominates. The PMA does not contain a methyl group in the


Fig. 4. Molecular mass distribution curves for GPC analysis

T a b l e 2. Average molecular masses and dispersity index of synthesized acrylic resins

Sample	M_n Da	M_w Da	\bar{D}
GMA/7MMA	8 315	15 040	1.64
GMA/6.5MMA/0.5BA	7 743	14 535	1.95
GMA/6MMA/BA	7 661	14 523	1.89
GMA/5MMA/2BA	7 391	16 670	2.15
2GMA/6MMA/BA	7 823	14 536	1.94
3GMA/6MMA/BA	7 792	14 625	1.87

main chain, so a termination reaction by recombination is more possible [23]. In the synthesis of acrylate resin, derivatives of acrylate and methacrylate monomers were used. Based on the molecular weight distribution curves shown in Figure 4, we can conclude that the synthesized acrylic resins were characterized by a similar narrow molecular weight distribution.

Chemical structure of oligo(meth)acrylic resin

To confirm the structure of the acrylate resin consisting of glycidyl methacrylate, methyl methacrylate and *n*-butyl acrylate, ¹H-NMR and FTIR spectra were recorded. Figure 5 shows ¹H-NMR spectra. The range of 0.84–1.07 ppm (assigned as 'G') is characteristic of the methyl groups derived from a chain of *n*-butyl acrylate [24]. The signal for the methyl groups derived from the main polymer chain is observed at 1.21–1.48 ppm (assigned as 'A'). The signals of aliphatic methylene groups (assigned as 'B', 'F', 'K', 'E') are found in the range 1.56–2.03 ppm [25]. The protons of epoxy groups derived from glycidyl methacrylate (assigned as 'I') appear in the range of 2.63–2.87 ppm, as a characteristic doublet of two hydrogen atoms adjacent to oxygen (-OCH₂-) [26]. The signal at 3.23 corresponds to (-CH-) of epoxy group (assigned as 'J') [26]. The most shifted proton resonance of the epoxide group is seen in the range of 3.72–4.48 ppm (assigned as 'H') [26]. The signal at 3.57 ppm (assigned as 'C') is characteristic for the methyl group (-O-CH₃) [27]. The resonance at 3.75 ppm (assigned as 'D') can be attributed to the aliphatic group (-OCH₂-) of *n*-butyl acrylate [25]. Other signals originate from unreacted monomers (in the range of 5.5–6.5 ppm) and solvent which was deuterated chloroform CDCl₃ (signal at 7.27 ppm) [24]. Unreacted monomers contribute to subsequent defects on surface such as craters or pin holes. For this reason, after pouring the resin into the PTFE mold, it was placed in an oven at 80°C for an hour.

The FTIR spectra are presented in Figure 6. The characteristic absorption stretching band for epoxy group (-C-O-C-) was found in the range of 950–860 cm⁻¹. At 2994 cm⁻¹, the band of C-H stretching vibration of aliphatic chain is observed. The absorptions at 1775 cm⁻¹ (C=O) and 1146 cm⁻¹ (C-O) are characteristic of acrylate resin. Other peaks in the range 1400–1500 cm⁻¹ derives from CH₂ scissor vibration [26].

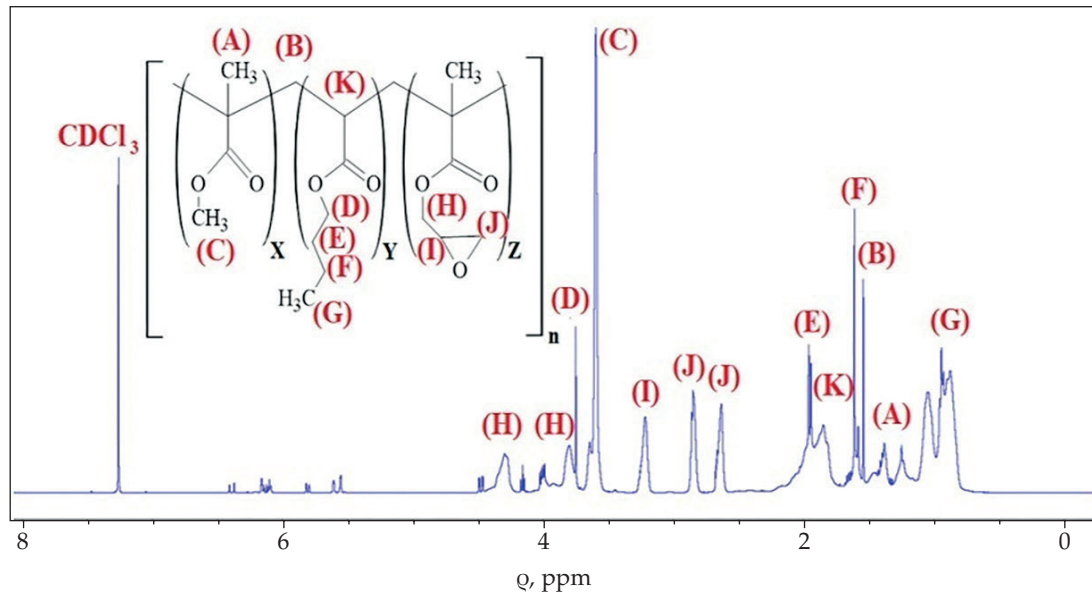
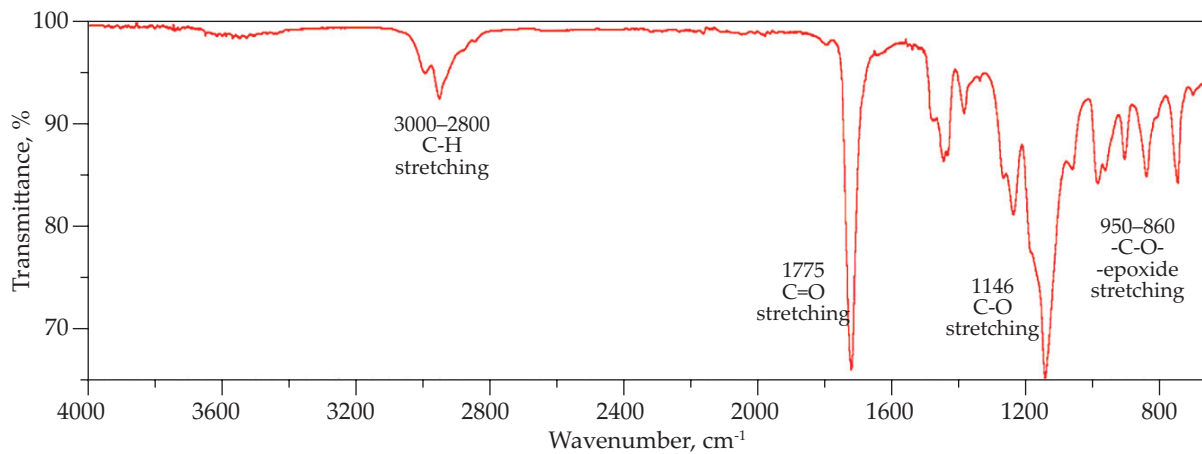
Fig. 5. ^1H NMR spectrum of GMA/6MMA/BA resin

Fig. 6. The FTIR spectra of GMA/6MMA/BA resin

Influence of chemical structure of the resin on formulation parameters

Once the chemical structure and the molar mass of the resins have been verified, a very important parameters affecting the formulation and storage stability of powder transparent coatings are viscosity and the glass

transition temperature (T_g). If the viscosity is too low, the powder sticks together. If the viscosity is too high, the coating melt on flow and there will be a problem with forming of a thin film. The molecular mass distribution and polydispersity are closely correlated with viscosity. Thermoplastic powder coatings are characterized by their high molecular weight and high viscosity. Among

T a b l e 3. Selected properties of the samples

Sample	Resin		Coating								
	Viscosity Pa·s	T_g °C	Thickness μm	Gloss for the angle of 60deg GU	Roughness, μm		Pressability mm	Scratch resistance g	Adhesion to the steel 0-5 scale	Relative hardness	Water contact angle °
					R_a	R_z					
GMA/7MMA	68	66	67.3±1.3	44.2±1.1	1.4±0.04	6.6±0.15	2.5±0.1	300±50	2	0.56±0.03	89.3±1.3
GMA/6.5MMA/0.5BA	57	52	78.7±1.5	81.0±0.9	1.1±0.02	5.2±0.12	2.7±0.2	450±50	2	0.57±0.02	93.3±2.4
GMA/6MMA/0.5BA	44	46	79.0±1.2	87.1±0.7	0.8±0.02	3.3±0.18	3.1±0.2	400±50	1	0.59±0.01	95.4±1.7
GMA/5MMA/2BA	37	21	75.2±1.6	93.7±1.1	0.6±0.03	3.0±0.13	4.8±0.1	500±50	0	0.64±0.02	97.5±2.1
2GMA/6MMA/BA	40	37	62.8±1.9	82.35±0.7	0±0.01	7.6±0.17	4.5±0.2	550±50	1	0.68±0.02	88.2±1.2
3GMA/6MMA/BA	38	31	72.3±1.7	85.9±0.8	0.7±0.01	3.8±0.14	3.2±0.2	500±50	1	0.59±0.02	83.2±1.5

other things, the problem with such systems is the application of a thin film. Thermosetting resin and UV-cured powder coatings are distinguished by lower molecular mass than that of thermoplastic systems (molecular mass in the range between 10 000 and 200 000 Da) [28]. This makes it possible to obtain a thin film and good physical-mechanical parameters. A thick coating can limit the access of light to the deepest layers and prevent the UV-curing process.

The viscosity at 140°C of the obtained acrylate resins was in the range of 37 to 69 Pa·s (cone rotation speed of 110 rpm) using a Brookfield viscometer (Table 3). The most optimal viscosity were GMA/6MMA/BA and 2GMA/6MMA/BA, because during application the powder didn't stick together, and the coatings were characterized by good flow. Other coatings which containing these resins were indicated worse or better flow and physic-mechanical properties, depending on the resin's composition.

The resin containing the most MMA has the highest viscosity. Viscosity decreases as BA and GMA content increases. The presence of methyl groups in the α -position of vinyl resulted in an increase in viscosity. Butyl acrylate contributes to decreasing of the viscosity of powder compositions, because it contains an aliphatic four-carbon chain. Too high viscosity causes problems with the formation of a thin film. Thick films are difficult to be cured by UV radiation. The resin with too high viscosity could be problematic with the surrounding pigments, fillers etc. to produce pigmented powder coatings.

The glass transition temperature (T_g) is also correlated to the structures of the polymer and viscosity. The values of T_g for oligo(meth)acrylic are shown in Table 3. Their excessively low values significantly limit the production of powder compositions, due to the difficulty in grinding, spraying and storage. For these reasons, the recommended minimum binder T_g values for powder coatings are 40°C in Europe and 45–50°C in North America [19]. From the synthesized resins, GMA/7MMA sample had the highest T_g , while GMA/5MMA/2BA is characterized by the lowest T_g value. In the case of GMA/5MMA/2BA sample, the powder sticks together after grinding. Based on the T_g , oligo(meth)acrylic resins were selected. The increase in GMA content also accelerates the transition from the glassy state to the elastic state below 40°C. The optimal amount of GMA was found for the resin with $T_g=45.9^\circ\text{C}$, in which molar ratio GMA:MMA:BA was 1:6:1. The increased amount of (BA), reduces the T_g , similarly to viscosity.

Thermal stability of materials has a very important practical significance for their research and development and quality control in production. When using resins for powder coatings, their thermal stability at the powder coating curing process, classically at 180–200°C, is very important. One of the methods characterizing the stability of materials is thermal analysis, which was used to assess the stability of the tested acrylic resins. Fig. 7 shows a TG and DTG thermograms of the 3GMA/6MMA/BA

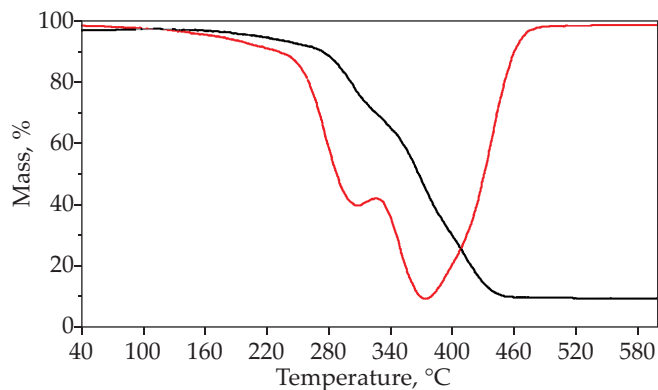


Fig. 7. TG (black curve) and DTG (red curve) thermograms of the 3GMA/6MMA/BA resin

resin. The mass loss of the resin sample changes with temperature, and the initial decomposition temperature of the resin is about 160°C. The weight loss in the initial stage is slow and is due to the volatilization or decomposition of a small amount of low molecular weight substances with the increase of heating rate [29]. At temperatures above 180°C, the weight loss begins to increase. The thermogravimetric weight loss of the resin can be divided into two stages. The first one with the maximum mass loss rate at 300°C and the second one with the maximum rate at 370°C. In the first stage of weight loss in the range of 180–320°C, the decomposition reaction of the resin is intense, and its rate is high, which may be due to the radical depolymerization where the chain backbone of the polymer is split by a radical reaction mechanism, with the main reaction products being the monomers [30]. The first step at 300°C corresponds to the end-chain β scission, followed at 370°C by a degradation initiation based on random (H-T) fission of the resin molecules [31]. Different mechanisms of thermal decomposition of acrylic polymers have been reported in the literature [32] proving that their degradation can be initiated by the thermally weak bonds, such as the head-to-head linkages, promoting facile homolytic scission of the chain around 270–300°C [33]. The further degradation at higher temperatures (350–400°C) is attributed to the chain-end depolymerization process [34] which is replaced by random chain-scission and depolymerization at over 400°C. Moreover, the solid residue at 500°C was around 0.6%.

Similarly, to results other researchers [16], TA tests showed that the thermal decomposition of the tested acrylic resins begins at a temperature of 180°C. If these resins will use for classic powder coatings formulation curing at 180°C, may decompose during the cross-linking process of the coating, which may result in worse performance properties. To prevent the decomposition of the resin during the cross-linking process, it is recommended to use them for low-temperature powder coatings or cross-linked during UV radiation.

To compare the obtained acrylic resins with industrial resins, the epoxy equivalent weight (EEW) was

determined. This parameter characterizes the number of epoxy groups in the resin. The epoxy value is defined as the number of moles of the epoxy group per 100 g of resin. The obtained EEWs are in the range of 500–900 g/eq. As the concentration of GMA increases, the EEW increases. The EEWs and T_g of the resulting acrylic resins are comparable to that of commercial polymer. The Almatex AP4411 type of GMA acrylic resin is characterized by 490–540 g/eq EEWs and the T_g is in the range of 40–60°C [35].

Influence of chemical composition and curing conditions on the UV-cured process

In the present study, cationic photopolymerization was used for UV-curing of the powder coatings. The UV-cured powder coatings were obtained by the reaction of epoxy groups derived from glycidyl methacrylate with the photoinitiator triaryl sulfonium hexafluorophosphate. The photoinitiator, which absorbs UV radiation and initiates crosslinking of powder coatings is an important component of the UV-cured powder coatings. The amount and type of photoinitiator was selected based on DMA research. In the cationic photopolymerization, the photoinitiation step usually uses onium salts of very strong acids, such as: iodonium, sulfonium, phosphonium and pyridinium salts [36]. This type of photoinitiators consists of an organic cation combined with an inorganic anion. Irradiation of diaryliodonium and a triaryl sulfonium salt yields strong acids with corresponding counter anions, as well as radical cations, which then initiate cationic polymerization [25, 37]. The cationic part of the photoinitiator is the light-absorbing component, which determines the thermal stability of the onium salt. The anionic moiety also influences the nature and reactivity of the propagating ion in polymerization and has a direct effect on polymerization kinetics. These salts contain inorganic parts such as PF_6^- , BF_4^- , SbF_6^- , AsF_6^- . Their reactivity in the photopolymerization process is related to the nucleophilicity and size of the corresponding anions and decreases in the order: $\text{SbF}_6^- > \text{AsF}_6^- > \text{PF}_6^- > \text{BF}_4^-$ [38].

The cationic photopolymerization was started when the plates were placed on a UV line. Depending on the generated UV radiation, the photoinitiator was selected based on the absorption spectrum. The common light sources are based on mercury lamps or LED (light

emitting diode) technology [39]. Another advantage of UV-induced polymerization is the possibility of in-line coatings on the conveyor system. In this work, the used light source was Dymax UVC-5 Compact Light-Curing Conveyor System equipped with a mercury lamp (high-power lamp 850 W). The wavelengths of UV radiation ranged from <300 and 365 nm. The triaryl sulfonium hexafluorophosphate has an absorption spectrum in the 360–380 nm range [40]. The number of cycles performed depended on the epoxy content in the acrylate resin. For this purpose, the test of polymerization was carried out (Table 4). When the powder coating was not dissolved under the influence of a MEK (methyl ethyl ketone) soaked cotton swab, after 30 times of wiping back and forth, the UV-cured process was completed. The polymerization test was carried out according to the standard in the “Technical requirements of the QUALICOAT quality label” [19]. One exposure cycle under the UV lamp lasted 7 s.

The L_3GMA/6MMA/BA powder transparent coating had the lowest number of cycles, but then the powder coating started turning yellow. The yellowing process leads to the degradation of the polymer, which results in a worsening of the mechanical properties. If the number of cycles is too high, the UV-curing time increases, which in turn increases energy consumption, which negatively affects process economics and sustainability. Nevertheless, these powder transparent coatings based on the epoxy group-containing acrylic resin are characterized by a faster curing speed and higher photopolymerization activity than polyurethane acrylate (PUA). For example, Qin *et al.* developed PUAs, when C=C conversion reaches around 85%, the curing time is at least 1 min [41].

A broader specification of UV-cured powder coatings was conducted using dynamic mechanical analysis (DMA). This technique was used to obtain information about the crosslink density (CD) of the UV-cured powder transparent coatings. The CD gave information about the physical and mechanical properties of the powder coatings, because the higher storage modulus and higher T_g , the properties also will be better. The modulus in the rubbery plateau (E'_{min}) of the cure was used to estimate the CD of the powder transparent coatings. The CD is related to the shear modulus in Equation (2) where R is the gas constant (8.314 J/mol K), T is the temperature (K) at which E' was measured and v_e is the number of moles of elastically effective network chains (mol/m^3) per volume in the film.

$$v_e = \frac{E'}{3RT} \quad (2)$$

The DMA curves of the powder transparent coatings are presented in Figures 8 and 9. Firstly, the effect of the concentration of the epoxy groups on the CD was checked at a constant concentration of the photoinitiator (2%) (Fig. 8). The highest CD was shown

Table 4. Number of cycles after which the powder transparent coatings were UV cured, using the polymerization test

Sample	Number of cycles
L_GMA/7MMA	20
L_GMA/6.5MMA/0.5BA	18
L_GMA/6MMA/BA	18
L_GMA/5MMA/2BA	16
L_2GMA/6MMA/BA	10
L_3GMA/6MMA/BA	8

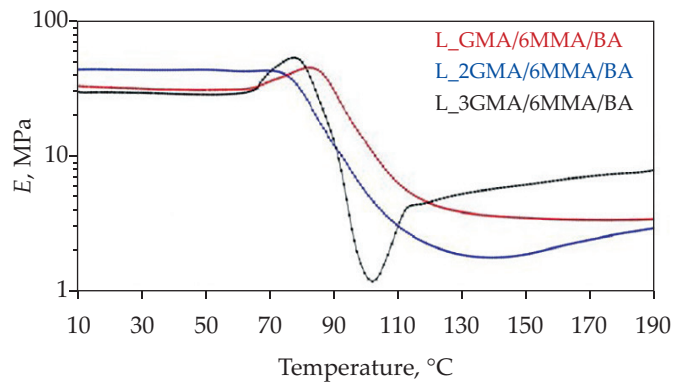


Fig. 8. DMA curves of L_GMA/6MMA/BA, L_2GMA/6MMA/BA and L_3GMA/6MMA/BA powder transparent coatings

by the coating L_2GMA/6MMA/BA (564.14 mol/m^3). The coatings L_GMA/6MMA/BA (167.47 mol/m^3) and L_3GMA/6MMA/BA (109.57 mol/m^3) were characterized by lower CD parameters. From these results, it can be concluded, that too small or too large concentration of epoxy groups can deteriorate the CD of the powder transparent coatings. The L_3GMA/6MMA/BA sample was cured after eight cycles but started to turn yellow. For

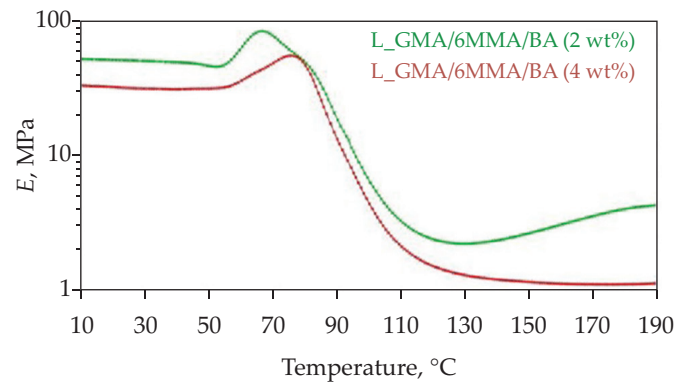


Fig. 9. DMA curves of L_GMA/6MMA/BA containing 2 wt% and 4 wt% of photoinitiator

this reason, L_2GMA/6MMA/BA sample was selected as a the best crosslinked.

Another important factor in the UV curing reaction is the concentration of the photoinitiator. Depending on the concentration of the used photoinitiator (2 wt% and 4 wt% triaryl sulfonium hexafluorophosphate) to the acrylic resin (based on GMA/6MMA/BA), the cross-link density increased from 167.47 mol/m^3 (2 wt%) to

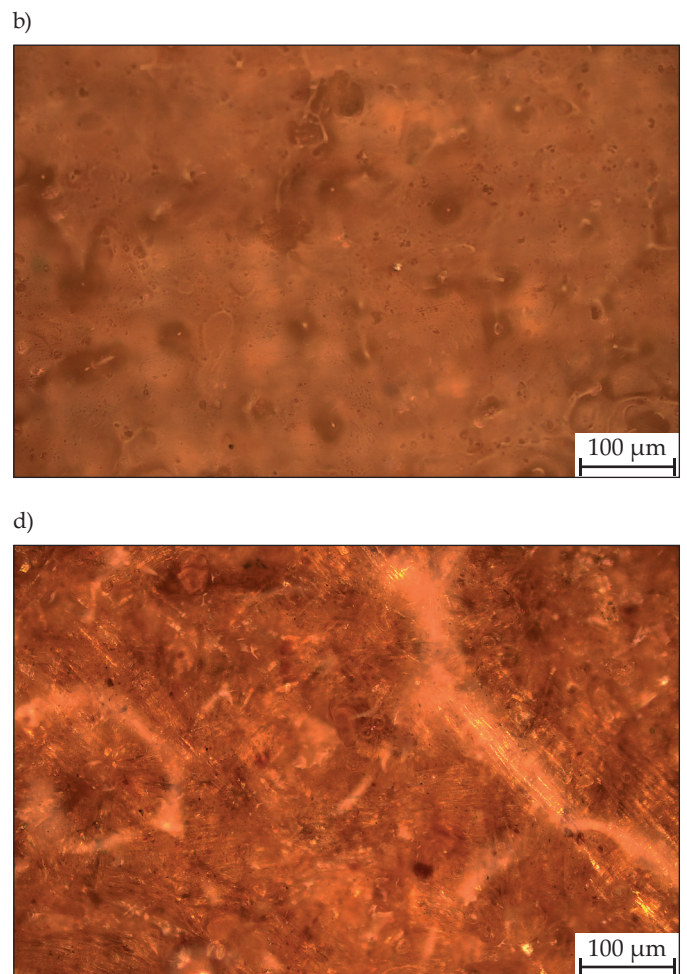
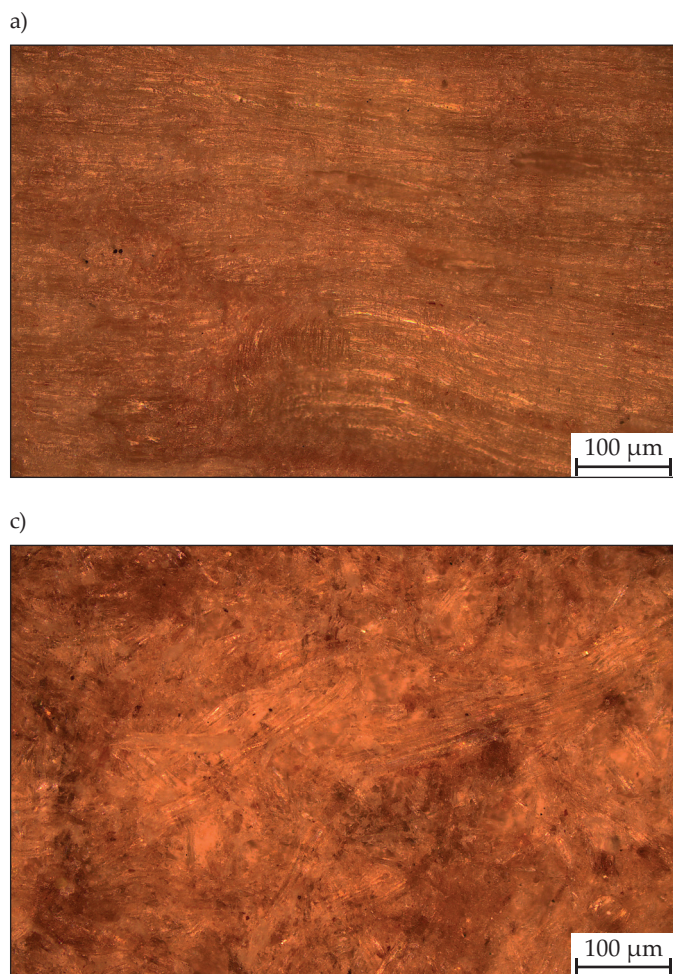


Fig. 10. Structure of heat-sensitive substrates without/with transparent powder coatings covered with L_GMA/6MMA/BA: a) wood without powder transparent coating, b) MDF panel without powder coating, c) wood coated with powder coating, d) MFD panel coated with powder coating

359.14 mol/m³ (4 wt%) (Fig. 9). If the concentration of photoinitiators were kept too low, photocurable coating materials could be uncured. The uncured coatings may result in the deterioration of mechanical properties and reduced thermal stability of the finished product. On the other hand, if the concentration of the photoinitiator is too high, shrinkages of the coatings are visible. Therefore, in this work 2 wt% was chosen as the optimum concentration of triaryl sulfonium hexafluorophosphate. The powder transparent coatings containing 2 wt% of photoinitiator did not have defects like orange peel, craters, and pinholes, compared to the coatings containing 4 wt%. Comparing the above results with the results from the literature, these powder coatings were characterized by high storage modulus [42].

Influence of chemical composition on the properties and application of UV-cured powder coatings

Recently, the important part of the UV-cured coatings manufacturing was development of wood, MDF or plastic coating. UV-curing provides advantages such as instant drying, coating of heat sensitive substrates, high curing rate, low space, and capital requirement for curing equipment [43]. To confirm these advantages of applying UV-cured powder transparent coatings based on oligo(meth)acrylic resins to heat-sensitive materials, the coatings on wood and MDF panels were prepared (Fig. 10). IR radiation was used to heating wood and MDF panels, because these substrates had low conductivity, which limits electrostatic application. Using a metallographic microscope, the wood and MDF were checked for degradation a temperature of 130°C and UV radiation. The pictures confirmed the absence of surface defects after exposure to a temperature of 130°C. The coatings applied to MDF, and wood were characterized by good mechanical properties. In addition, the developed fast curing powder coatings ensure that the absorption of coatings by the wood surface is minimized without reducing adhesion properties.

Another parameter influencing the UV curing process is the thickness. The photopolymerization mechanism is reduced when the coating is too thick. UV rays cannot pass through to the lower layers of the coatings [44]. In addition, an important issue is whether a pigment was added to the prepared powder transparent coatings. In cationic photopolymerization, the thickness is not as important as for free-radical photopolymerization. Cationic photopolymerization proceeds ionically. For this reason, the coating is cured uniformly. Nevertheless, the thickness of the powder coatings must comply with standards.

The obtained powder coatings ranged in thickness from 60 to 80 μm measured by using micro-tri-gloss μ tester from BYK-Gardner according to the standards: PN-EN ISO 2306 and "Technical requirements of the QUALICOAT quality label" [19]. The checked physical-mechanical properties are listed in Table 3.

According to the Qualicoat requirements, the obtained powder transparent coatings exhibited gloss except for L_GMA/7MMA, which is semi-gloss. Gloss of the coatings decreases with increasing roughness. The increasing roughness of powder coatings can be a consequence of the higher viscosity. High viscosity was due to the high concentration of MMA in the powder composition. Replacing of MMA with the same number of moles of BA significantly increases the gloss and cupping. The BA contains a four-carbon aliphatic chain, contributing to increased flexibility and adhesion to the surface. Unfortunately, too much of *n*-butyl acrylate causes instability in the final product. Methyl methacrylate increases stiffness but reduces flexibility in comparison with the homologous acrylate's monomer. Methacrylate's can also increase elasticity. As the side chain of methacrylate's becomes longer, elasticity increases. However, when the side chain length is up to 8 (acrylic) and up to 12 carbon atoms (methacrylate's), elasticity decrease. With longer chains, the decrease in elasticity is due to the increase in their crystallinity [20]. The crosslinking density and GMA content also influence the mechanical properties. Too high crosslinking density is detrimental to cracking resistance, as little plastic deformation can take place in such materials and residual stresses. Therefore, such coatings may be characterized by low scratch resistance, pressability, and adhesion to the steel. The L_2GMA/6MMA/BA powder coating demonstrated the highest crosslink density, and the properties of the coating were satisfying. This powder transparent coating indicated good scratch resistance and hardness compared to other samples. The water contact angle allows the characterization of the hydrophobic or hydrophilic character of the coatings. Increasing in the epoxy groups content resulted in a decrease in the hydrophobicity of the coating. The increase in the hydrophobicity of the coating was influenced by the monomers containing nonpolar groups: methyl group (-CH₃) derived from methyl methacrylate, glycidyl methacrylate and butyl group derived from butyl acrylate. An increase in the water contact angle indicates an increase in the water resistance of the coatings.

CONCLUSIONS

The objective of the study was to investigate the influence of the chemical structure and the radiation curing parameters of the UV-cured powder transparent coatings based on oligo(meth)acrylic resins on the properties of powder coatings. Examination of these relationships is very important to optimize the process in terms of obtaining coatings with the best properties.

The chemical structure of the oligo(meth)acrylic resins containing methyl methacrylate, *n*-butyl acrylate and glycidyl methacrylate and their different molar ratios has been investigated. NMR and FTIR spectra confirmed the expected structure of the acrylate resins. The average molecular weights of the resins were in the range of 7000–8000 Da and did not significantly depend on the molar

ratio of the monomers used. Based on the viscosity and glass transition temperature, it was possible to predict whether a powder coating will be thermally stable during storage and that the powder will not stick together. The methyl methacrylate used in the synthesis is characterized by a rigid structure, due to the methyl group ($-CH_3$) in the main chain at the α position to the carbonyl group. For this reason, MMA increased thermal stability, viscosity, and hardness of the coatings. Butyl acrylic give flexibility and improved properties such as: cupping, gloss, and water contact angle. With the increase of the *n*-butyl acrylate content in the resin, T_g and the viscosity of resin decreased, which consequently affects the final properties of the powder coating. The value of viscosity and glass transition temperature, and physical properties allowed us to determine the most optimal molar ratio to MMA and BA content in the resin (6 MMA: 1BA).

GMA was used as a major monomer, because the epoxy functional group reacted with a photoinitiator (triaryl sulfonium hexafluorophosphate) and polymerized by cationic photopolymerization mechanism. The photoinitiated cationic polymerization allows to obtain UV-cured powder transparent coatings based on acrylate resin. DMA analysis showed that the optimization of the content of the functional epoxy group and photoinitiator played an important role in the UV curing process. The powder coating L_2GMA/6MMA/BA prepared by using 2 wt% triaryl sulfonium hexafluorophosphate was characterized by the highest crosslink density and the good curing time (10 cycles under UV lamp, 1 cycle = 7 s, total time 70 s). Considering the adjustable parameters such as molecular weight, T_g and crosslink density, optimal parameters were obtained. This powder transparent coatings were also characterized by good physic-mechanical properties such as: pressability, scratch resistance, and hardness.

UV-cured powder coatings cured by cationic photopolymerization are a new approach to the powder coatings market and give many benefits such as energy and time savings and environmental friendliness by avoiding solvent exposure. The properties and applications of the coatings strongly depend on their chemical composition and process conditions. On the other hand, the selection, or settings of the exposure systems, such as lamp spectrum, light intensity, or exposure time, depends on the choice of components.

The application of UV-cured powder coating increases the benefits over thermosetting coatings. Of course, UV-cured powder coatings also have disadvantages e.g. investment of UV equipment and material costs. But the advantages of UV-cured powder coatings outweigh the one-time equipment investment costs and may lead to a new approach for powder coatings formulation. The UV-cured powder coatings based on cationic photopolymerization mechanism can be applied on wood and MDF panels, which broadens the scope of their applications. A faster curing process with lower temperature requirements leads to low energy consumption. Moreover, UV-

curing cationic photopolymerization process does not need inert gas during the process because lack of the oxygen inhibition.

ACKNOWLEDGEMENT

This work was supported by the Podkarpackie Innovation Center (PCI) under grant No. N3_103, contract No. 68/PRZ/1DG/PCI/2021.

The author thanks Evonic Degussa GmbH and Byk for sending free samples of raw materials.

REFERENCES

- [1] Pilch-Pitera B., Byczynski Ł., Mysliwiec B.: *Progress in Organic Coatings* **2017**, 113, 82. <https://doi.org/10.1016/j.porgcoat.2017.08.011>
- [2] Pilch-Pitera B.: *Progress in Organic Coatings* **2014**, 77, 1653. <https://doi.org/10.1016/j.porgcoat.2014.05.021>
- [3] V. Mannari V., Patel C.J.: "Understanding Coatings Raw Materials", Vincentz Network GmbH, Hannover 2015.
- [4] Johansson M., Falken H., Irestedt A. *et al.*: *Journal of Coatings Technology* **1998**, 70, 57. <http://doi.org/10.1007/bf02697841>
- [5] Li C., Johansson M., Buijsen P. *et al.*: *Progress in Organic Coatings* **2021**, 151, 106073. <https://doi.org/10.1016/j.porgcoat.2020.106073>
- [6] Deng L., Tang L., Qu J.: *Progress in Organic Coatings* **2020**, 141, 105546. <https://doi.org/10.1016/j.porgcoat.2020.105546>
- [7] Yagci Y., Jockusch S., Turro N.J.: *Macromolecules* **2010**, 43(15), 6245. <https://doi.org/10.1021/ma1007545>
- [8] Christmann J., Ley C., Allonas X. *et al.*: *Polymer* **2019**, 160, 254. <https://doi.org/10.1016/j.polymer.2018.11.057>
- [9] Shi Y., Yan C., Zhou Y. *et al.*: "Materials for Additive Manufacturing", Academic Press, Cambridge 2021.
- [10] Michaudel Q., Kottisch V., Fors B.P.: *Angewandte Chemie International Edition* **2017**, 56(33), 9670. <https://doi.org/10.1002/anie.201701425>
- [11] Czachor-Jadacka D., Pilch-Pitera B., M. Kisiel M. *et al.*: *Materials* **2021**, 14(16), 4710. <https://doi.org/10.3390/ma14164710>
- [12] *Pat. DE 1 016 382 6A1* (2003).
- [13] Hammer T.J., Mehr H.M.S., Pugh C. *et al.*: *Journal of Coatings Technology and Research* **2021**, 18, 333. <https://doi.org/10.1007/s11998-020-00391-8>
- [14] Rawat R.S., Chouhan N., Talwar M. *et al.*: *Progress in Organic Coatings* **2019**, 135, 490. <https://doi.org/10.1016/j.porgcoat.2019.06.051>
- [15] Wu C., Meng B.C., Tam L. *et al.*: *Polymer Testing* **2022**, 114, 107708. <https://doi.org/10.1016/j.polymertesting.2022.107708>
- [16] Chebil M.S., Gerard P., Issard H. *et al.*: *Polymer Degradation and Stability* **2023**, 213, 110367. <https://doi.org/10.1016/j.polymdegradstab.2023.110367>

- [17] <https://www.pcimag.com/articles/85628-uv-curable-powder-coatings-benefits-and-performance> (access date 24.07.2023)
- [18] *Pat. US* 8 09 768 7B2 (2009).
- [19] Bellot P.: "Specifications for a quality label for liquid and powder coatings on aluminum for architectural applications", QUALICOAT Specifications, Zurich 2021.
- [20] Poth U., Schwalm R., Schwartz M. *et al.*: "Acrylate Resins", Vincentz Network GmbH, Hanover, 2011.
- [21] Fink J.K.: "Reactive Polymers Fundamentals and Applications", Elsevier Science, Amsterdam 2013.
- [22] Taheri M., Jahanfar M., Ogino K.: *Designed Monomers and Polymers* **2019**, 22, 213.
<https://doi.org/10.1080/15685551.2019.1699349>
- [23] Jones F., Nichols M.E., Pappas S. P.: "Organic Coatings Science and Technology, 4th edition", Wiley, Hoboken 2017.
- [24] Sugumaran D., Karim K.J.A.: *eProceedings Chemistry 2* **2017**, 1.
<https://doi.org/10.13140/RG.2.2.33911.93601>
- [25] Brar A.S., Pradhan D.R., Hooda S.: *Journal of Molecular Structure* **2004**, 699(1–3), 39.
<https://doi.org/10.1016/j.molstruc.2004.03.055>
- [26] Hayek A., Xu Y., Okada T. *et al.*: *Journal of Materials Chemistry* **2008**, 28, 3316.
<https://doi.org/10.1039/b809656b>
- [27] Babaç C., Güven G., David G. *et al.*: *European Polymer Journal* **2004**, 40(8), 1947.
<https://doi.org/10.1016/j.eurpolymj.2004.03.004>
- [28] Spyrou E.: "Powder Coatings Chemistry and Technology", Vincentz Network GmbH, Hanover 2014.
- [29] Zhuxin L., Xue L., Zhaoxian C. *et al.*: *Progress in Organic Coatings* **2022**, 172, 107101.
<https://doi.org/10.1016/j.porgcoat.2022.107101>
- [30] Gkaliou K., Benedini L., Sárosy Z. *et al.*: *Waste Management* **2023**, 164, 191.
<https://doi.org/10.1016/j.wasman.2023.04.007>
- [31] Moens E.K.C., De Smit K., Marien Y.W. *et al.*: *Polymers* **2020**, 12(8), 1667.
<https://doi.org/10.3390/polym12081667>
- [32] Kashiwagi T., Inaba A., Brown J.E. *et al.*: *Macromolecules* **1986**, 19(8), 2160.
<https://doi.org/10.1021/ma00162a010>
- [33] Ferriol M., Gentilhomme A., Cochez M. *et al.*: *Polymer Degradation and Stability* **2003**, 79(2), 271.
[https://doi.org/10.1016/S0141-3910\(02\)00291-4](https://doi.org/10.1016/S0141-3910(02)00291-4)
- [34] Peterson J.D., Vyazovkin S., Wight C.A.: *The Journal of Physical Chemistry B* **1999**, 103(38), 8087.
<https://doi.org/10.1021/jp991582d>
- [35] https://www.andersondevelopment.com/view_width/Acrylate-Resins/Properties-of-Almatex-Coating-Resins/65 (access date 20.01.2023)
- [36] Sangermano M., Roppolo I., Chiappone A.: *Polymers* **2018**, 10(2), 136.
<https://doi.org/10.3390/polym10020136>
- [37] Wang D., Szillat F., Fouassier J.P. *et al.*: *Macromolecules* **2019**, 52(15), 5638.
<https://doi.org/10.1021/acs.macromol.9b00952>
- [38] Dadashi-Silab S., Doran S., Yagci Y.: *Chemical Reviews* **2016**, 116(17), 10212.
<https://doi.org/10.1021/acs.chemrev.5b00586>
- [39] <https://www.pfonline.com/articles/uv-cured-powder-coatings-and-led-curing-technology>, 2019 (access date 5.02.2023)
- [40] <https://polymerinnovationblog.com/uv-curing-part-2-tour-uv-spectrum/> (access date 18.01.2016)
- [41] Qin L., He Y., Liu B. *et al.*: *Progress in Organic Coatings* **2013**, 76(11), 1594.
<https://doi.org/10.1016/j.porgcoat.2013.07.005>
- [42] Kardar P., Ebrahimi M., Bastani S.: *Pigment and Resin Technology* **2014**, 43(4), 177.
<https://doi.org/10.1108/PRT-07-2013-0054>
- [43] Wang F., Hu J.Q., Tu W.P.: *Progress in Organic Coatings* **2008**, 62(3), 245.
<https://doi.org/10.1016/j.porgcoat.2007.12.005>
- [44] Park J.W., Sim K.B., Back J.H. *et al.*: *Materials and Design* **2019**, 178, 107855.
<https://doi.org/10.1016/j.matdes.2019.107855>

Received 3 XI 2023.

